

Parton energy loss in glasma

P. Aurenche^a and B.G. Zakharov^b

^a *LAPTH, Université de Savoie, CNRS,
BP 110, F-74941, Annecy-le-Vieux Cedex, France*

^b *L.D. Landau Institute for Theoretical Physics, GSP-1, 117940,
Kosygina Str. 2, 117334 Moscow, Russia*

Abstract

We study the synchrotron-like gluon emission in AA -collisions from fast partons due to interaction with the coherent glasma color fields. Our results show that for RHIC and LHC conditions the contribution of this mechanism to parton energy loss is much smaller than the radiative energy loss in the plasma phase.

1 Introduction

It is widely believed that the observed large suppression of high- p_T hadrons in AA -collisions at RHIC and LHC (the so-called jet quenching (JQ)) is due to parton energy loss in the quark-gluon plasma (QGP). The observation of this phenomenon and successful hydrodynamic description of hadron production at low p_T are the strongest arguments for formation of the QGP in heavy-ion collisions at RHIC and LHC. In pQCD partons lose energy mostly through the induced gluon emission due to multiple scattering in the QGP [1, 2, 3, 4, 5, 6], and a small fraction of the energy loss comes from the elastic collisions [7, 8]. At RHIC and LHC, the entropy of the QGP required to describe the observed suppression of high- p_T hadrons, within the pQCD calculations of the radiative and collisional energy losses [9, 10, 11], turns out to be qualitatively consistent with that obtained within the hydrodynamic simulations from the low- p_T data. This consistency looks very encouraging. However, one must keep in mind that the theoretical uncertainties both in the pQCD calculations of the JQ and in the hydrodynamic simulations are rather large. On the JQ side there remain open questions on additional mechanisms of the parton energy loss which can modify the picture with the dominating radiative energy loss in the QGP phase.

One of the potentially important energy loss mechanisms is the synchrotron-like gluon emission in the strong classical color fields in the initial pre-equilibrium stage of AA -collisions [12] predicted within the Color Glass Condensate (CGC) model [13, 14, 15, 16]. This stage (termed glasma [17]) is now under active investigation (see [18, 19] and references therein). However, its role in parton energy loss still has not been studied. The evaluation of the classical Yang-Mills fields in AA -collisions within the CGC model shows that just after the collision of the Lorentz contracted nuclei a system of the color flux tubes with the longitudinal boost invariant color electric and color magnetic fields

(with $|E_z| \approx |B_z|$) should be produced [20]. The typical transverse coherence length for the color fields in this phase is $\sim 1/Q_s$, where Q_s ($\sim 1 - 1.5$ GeV for RHIC and LHC conditions [21]) is the saturation scale of the nuclear parton distributions. At the proper time $\tau \sim 1/Q_s$ the strength of the glasma electric and magnetic longitudinal fields is $gE_z \sim gB_z \sim Q_s^2$ [20]. The transverse fields, which are absent at $\tau = 0$, are generated at later times and become close to the longitudinal ones at $\tau \gtrsim 1/Q_s$ [20, 22]. At such times the glasma energy density decreases $\propto 1/\tau$. At later times the thermalization of the glasma color fields should lead to formation of the equilibrium QGP, but the detailed mechanism for the thermalization remains unclear. Qualitative analyses say that the glasma thermalization goes probably via instabilities of the color flux tubes rising quickly at $\tau \gtrsim 1/Q_s$ [23, 22, 24]. They should lead to a fast randomization of the boost invariant glasma color fields at the time scale about 2–3 units of $1/Q_s$. This thermalization time agrees qualitatively with the hydrodynamic fits of the data on AA -collisions which favor the thermalization at $\tau_0 \sim 0.4 - 1$ fm [25, 26].

For RHIC-LHC conditions the typical Lorentz force acting on a fast parton crossing the glasma turns out to be very large $\sim Q_s^2 \sim 5 - 10$ GeV/fm. It is about 10–20 times that for the Debye screened color center in the QGP $\sim \alpha_s m_D^2$ (if one takes $\alpha_s \sim 0.3$ and $m_D \sim 0.5$ GeV). It raises a natural question about the impact of the glasma on the radiative energy loss. If one ignores the interaction of fast partons with the pre-equilibrium phase at all, then for jets with energies $\lesssim 100$ GeV the parton showering at $\tau \lesssim \tau_0 \sim 0.5 - 1$ fm can be viewed as almost pure DGLAP shower, and the interference of the DGLAP stage with the induced gluon emission in the bulk of the QGP at $\tau \gtrsim \tau_0$ should be relatively small [10]. Thus in this energy range the question of the glasma role in the JQ is equivalent to the question to what extent the glasma modifies the DGLAP gluon emission. The purpose of the present paper is to give a qualitative estimate of this effect.

2 Formulation of the model and basic formulas for the synchrotron-like gluon emission

An accurate calculation of the synchrotron-like gluon emission due to interaction of fast partons with the glasma is presently impossible. It would require a detailed understanding of the decay and thermalization of the glasma color flux tubes which remain unclear. However, since the strength of the color fields in the flux tubes decreases quickly, the transverse momentum which a fast parton gets in the glasma should mostly come from interaction with the coherent color field of the first crossed color flux tube. The effect of the random transverse momentum kicks which a fast parton undergoes in the glasma at later times should be small due to weakness of the fields and the destructive interference of the chaotic contributions from different color tubes. For the above reasons as a first step in understanding the influence of the glasma on parton energy loss it seems reasonable to consider a simple model with a uniform time-dependent color field which acts only for a limited range of τ about 2–3 units of $1/Q_s$.

So we will consider the synchrotron-like gluon emission from a fast parton (we choose the z -axis along the initial parton momentum) in a slab of thickness $L \sim (2 - 3)/Q_s$ with

the transverse chromoelectric, \mathbf{E}_a , and chromomagnetic, \mathbf{H}_a , fields (hereafter a denote the color index). We will ignore the longitudinal (along the jet) components of the color fields since similarly to the photon emission in QED their effect should be small for relativistic partons. For simplicity we assume that both the electric and magnetic fields are oriented to the same direction in the color space. It is enough to consider the color fields with nonzero components only in the Cartan subalgebra, i.e., for $a = 3$ and $a = 8$ for the $SU(3)$ color group.

We present our formulas for a fast quark produced in a hard process at central rapidity $y = 0$ (so the initial quark momentum and the z -axis of our coordinate system are perpendicular to the AA -collision axis). We take $z = 0$ for the production point. The starting point of our analysis is similar to the case of the synchrotron-like energy loss spectrum for a fast parton propagating in an infinite uniform color field addressed in [27]. We write the S -matrix element of the $q \rightarrow gq'$ transition as (we omit the color factors and indices)

$$\langle gq' | \hat{S} | q \rangle = -ig \int d^4y \bar{\psi}_{q'}(y) \gamma^\mu A_\mu^*(y) \psi_q(y), \quad (1)$$

where $\psi_{q,q'}$ are the wave functions of the initial quark and final quark, A_μ is the wave function of the emitted gluon.

For our choice of the external color field (which has only $a = 3$ and $a = 8$ nonzero components) it does not change the quark color state. However, it is not the case for gluons, which are rotated in the color space as they move in the color field. The interaction of the gluons with the background color field can be diagonalized by introducing the gluon fields having definite color isospin, Q_A , and color hypercharge, Q_B , (we will describe the color charge by the two-dimensional vector $Q = (Q_A, Q_B)$). In terms of the usual gluon vector potential, A_a , the diagonal color gluon states read (the Lorentz indices are omitted) $X = (A_1 + iA_2)/\sqrt{2}$ ($Q = (-1, 0)$), $Y = (A_4 + iA_5)/\sqrt{2}$ ($Q = (-1/2, -\sqrt{3}/2)$), $Z = (A_6 + iA_7)/\sqrt{2}$ ($Q = (1/2, -\sqrt{3}/2)$). The neutral gluons $A = A_3$ and $B = A_8$ with $Q = (0, 0)$, to leading order in the coupling constant, do not interact with the background field at all, and the emission of these gluons are similar to the photon radiation in QED.

We evaluate the matrix element (1) within the small angle approximation, i.e., we assume that for each parton its transverse momentum is small compared to the longitudinal one. We write each quark wave function in the form

$$\psi_i(y) = \frac{\exp[-iE_i(t-z)]}{\sqrt{2E_i}} \hat{u}_\lambda \phi_i(z, \boldsymbol{\rho}), \quad (2)$$

where the four-vector y is defined as $y^\mu = (t, \boldsymbol{\rho}, z)$ (hereafter the bold vectors denote the transverse vectors), λ is the quark helicity, \hat{u}_λ is the Dirac spinor operator. In the small angle approximation the z -dependence of the transverse wave functions ϕ_i is governed by the two-dimensional Schrödinger equation

$$i \frac{\partial \phi_i(z, \boldsymbol{\rho})}{\partial z} = \left\{ \frac{(\mathbf{p} - gQ_n \mathbf{G}_n)^2 + m_q^2}{2E_i} + U_i(z, \boldsymbol{\rho}) \right\} \phi_i(z, \boldsymbol{\rho}) \quad (3)$$

with the potential

$$U_i(z, \boldsymbol{\rho}) = gQ_n^i [G_n^0(z, \boldsymbol{\rho}) - G_n^3(z, \boldsymbol{\rho})]. \quad (4)$$

Here G_n^μ denotes the external vector potential (the superscripts are the Lorentz indexes and $n = 1, 2$ correspond to the A and B color components in the Cartan subalgebra), Q_n^i is the quark color charge.

We take the external vector potential in the form $G_n^0 = -\boldsymbol{\rho} \cdot \mathbf{E}_n$, $\mathbf{G}_n = 0$, and $G_n^3 = [\mathbf{H}_n \times \boldsymbol{\rho}]^3$, where \mathbf{E}_n and \mathbf{H}_n are the electric and magnetic fields. In this case the kinetic term in (3) does not contain the external vector potential at all, and the potential U_i can be written as

$$U_i(z, \boldsymbol{\rho}) = -\mathbf{F}_i \cdot \boldsymbol{\rho}, \quad (5)$$

where \mathbf{F}_i is the Lorentz force. The wave function of the emitted gluon can be represented in a similar way. In our numerical computations for the quark mass we take $m_q = 0.3$ GeV. However, the value of the quark mass is not very important. For the gluon mass we take $m_g = 0.75$ GeV. This value was obtained from the analysis of the low- x proton structure function F_2 within the dipole BFKL equation [28]. It agrees well with the natural infrared cutoff for gluon emission $m_g \sim 1/R_c$, where $R_c \approx 0.27$ fm is the gluon correlation radius in the QCD vacuum [29].

The solution of (3) can be taken in the form

$$\phi_i(z, \boldsymbol{\rho}) = \exp \left\{ i\mathbf{p}_i(z)\boldsymbol{\rho} - \frac{i}{2E_i} \int_0^z dz' [\mathbf{p}_i^2(z') + m_q^2] \right\}. \quad (6)$$

Here the transverse momentum $\mathbf{p}_i(z)$ is the solution to the classical parton equation of motion in the impact parameter plane

$$\frac{d\mathbf{p}_i}{dz} = \mathbf{F}_i(z). \quad (7)$$

By using (1), (2), (6) one can obtain

$$\begin{aligned} \langle gq' | \hat{S} | q \rangle &= -ig(2\pi)^3 \delta(\omega + E_{q'} - E_q) \int_0^\infty dz V(\mathbf{q}(z), \{\lambda\}) \delta(\mathbf{p}_g(z) + \mathbf{p}_{q'}(z) - \mathbf{p}_q(z)) \\ &\times \exp \left\{ i \int_0^z dz' \left[\frac{\mathbf{p}_g^2(z') + m_g^2}{2\omega} + \frac{\mathbf{p}_{q'}^2(z') + m_q^2}{2E_{q'}} - \frac{\mathbf{p}_q^2(z') + m_q^2}{2E_q} \right] \right\}, \quad (8) \end{aligned}$$

where ω is the gluon energy, V is the vertex factor, $\{\lambda\}$ is the set of the parton helicities. For the transition conserving quark helicity $V(\mathbf{q}, \lambda) = -iC[2\lambda_q x + (2-x)\lambda_g][q_x(z) - i\lambda_g q_y(z)]/[x\sqrt{2(1-x)}]$, and for the spin-flip case $V = ixm_q C(2\lambda_q \lambda_g + 1)/\sqrt{2(1-x)}$. Here $\mathbf{q}(z) = \mathbf{p}_g(z)(1-x) - \mathbf{p}_{q'}(z)x$, $x = \omega/E_q$, and $C = \lambda_{fi}^a \chi_a^*/2$ is the color factor (i, f are the color indexes of the initial and final quarks, χ_a is the color wave function of the emitted gluon). Due to the color charge conservation $\mathbf{F}_q = \mathbf{F}_g + \mathbf{F}_{q'}$. For this reason, the argument of the momentum δ -function on the right-hand part of (8) does not depend on z , and can be replaced by $\mathbf{p}_g^+ + \mathbf{p}_{q'}^+ - \mathbf{p}_q^+$, where $\mathbf{p}_i^+ = \mathbf{p}_i(\infty)$. Then, noting that the expression in the square brackets in (8) can be rewritten as $[\mathbf{q}^2(z') + \epsilon^2]/2M$ with $\epsilon^2 = m_q^2 x^2 + (1-x)m_g^2$ and $M = E_q x(1-x)$, the matrix element (8) can be rewritten as

$$\langle gq' | \hat{S} | q \rangle = -i(2\pi)^3 \delta(\omega + E_{q'} - E_q) \delta(\mathbf{p}_g^+ + \mathbf{p}_{q'}^+ - \mathbf{p}_q^+) T, \quad (9)$$

$$T = g \int_0^\infty dz V(\mathbf{q}(z), \{\lambda\}) \exp \left\{ i \int_0^z dz' \left[\frac{\mathbf{q}^2(z') + \epsilon^2}{2M} \right] \right\}. \quad (10)$$

With the help of the standard Fermi golden rule the gluon distribution in terms of the amplitude T can be written as

$$\frac{dN}{d\omega d\mathbf{q}} = \frac{|T|^2}{8(2\pi)^3 E_q^3 x(1-x)}. \quad (11)$$

Hereafter we do not show the averaging over the initial and summing over the final color/spin states. In the absence of the external color field the momentum $\mathbf{q}(z)$ in (10) does not vary with z and equals to the final momentum at $z = \infty$ (we will denote it \mathbf{q}). In this case (10) gives the vacuum amplitude

$$T_v = gV(\mathbf{q}, \{\lambda\}) \frac{2iM}{\mathbf{q}^2 + \epsilon^2}. \quad (12)$$

Substituting (12) into (11) we obtain the usual vacuum LO pQCD distribution for the $q \rightarrow gq$ splitting (hereafter we neglect the spin-flip part of the vertex ($\propto m_q$) which gives a negligible contribution)

$$\frac{dN_v}{d\omega d\mathbf{q}} = \frac{2C_F\alpha_s}{\pi^2 x E_q} \left(1 - x + \frac{x^2}{2}\right) \frac{\mathbf{q}^2}{(\mathbf{q}^2 + \epsilon^2)^2}. \quad (13)$$

For a nonzero external field we write the amplitude T as a sum

$$T = T_v + T_s, \quad (14)$$

where T_s describes the correction due to the external field. Since the momentum \mathbf{q} varies with z only at $z < L$, from (10) one can obtain

$$T_s = g \int_0^L dz V(\mathbf{q}(z), \{\lambda\}) \exp \left\{ i \int_0^z dz' \left[\frac{\mathbf{q}^2(z') + \epsilon^2}{2M} \right] \right\} - (\mathbf{q}(z) \rightarrow \mathbf{q}). \quad (15)$$

In terms of $T_{v,s}$ the synchrotron-like correction to the LO gluon spectrum (13) reads

$$\frac{dN_s}{d\omega d\mathbf{q}} = \frac{2\text{Re}(T_v T_s^*) + |T_s|^2}{8(2\pi)^3 E_q^3 x(1-x)}. \quad (16)$$

The glasma correction to the ω -spectrum can be obtained from (16) by integrating over the transverse momentum \mathbf{q} . Note that contrary to the LO vacuum spectrum (13), which $\propto 1/\mathbf{q}^2$ at large \mathbf{q}^2 and without a constraint on \mathbf{q}^2 gives a logarithmically divergent ω -spectrum, the \mathbf{q} -integral for the correction term is convergent at large \mathbf{q}^2 .

The ω -spectrum can also be obtained within the light-cone path integral (LCPI) approach [2] formulated in the impact parameter space. The LCPI formalism has originally been developed for gluon emission induced by multiple parton scattering. But it applies to the synchrotron-like gluon emission as well. In this case the LCPI gives for the ω -spectrum

$$\frac{dN_s}{d\omega} = 2\text{Re} \int_0^\infty dz_1 \int_{z_1}^\infty dz_2 \hat{g} [\mathcal{K}(\boldsymbol{\rho}_2, z_2 | \boldsymbol{\rho}_1, z_1) - \mathcal{K}_0(\boldsymbol{\rho}_2, z_2 | \boldsymbol{\rho}_1, z_1)] \Big|_{\boldsymbol{\rho}_1 = \boldsymbol{\rho}_2 = 0}. \quad (17)$$

Here \hat{g} is the vertex operator given by

$$\begin{aligned}\hat{g} &= \frac{\alpha_s}{8E_q^3 x(1-x)} \sum_{\{\lambda\}} V(-i\partial/\partial\boldsymbol{\rho}_1, \{\lambda\}) V^*(-i\partial/\partial\boldsymbol{\rho}_2, \{\lambda\}) \\ &= \frac{|C|^2 \alpha_s}{E_q^3 x^3 (1-x)^2} \left(1-x + \frac{x^2}{2}\right) \frac{\partial}{\partial\boldsymbol{\rho}_1} \cdot \frac{\partial}{\partial\boldsymbol{\rho}_2},\end{aligned}\quad (18)$$

\mathcal{K} is the Green's function of the Schrödinger equation with the Hamiltonian

$$\hat{H} = -\frac{1}{2M} \left(\frac{\partial}{\partial\boldsymbol{\rho}}\right)^2 - \mathbf{f} \cdot \boldsymbol{\rho} + \frac{\epsilon^2}{2M}, \quad (19)$$

and \mathcal{K}_0 is the Green's function for the Hamiltonian (19) with $\mathbf{f} = 0$. The Green's function for the Hamiltonian (19) is known explicitly (see, for example, [30])

$$\mathcal{K}(\boldsymbol{\rho}_2, z_2 | \boldsymbol{\rho}_1, z_1) = \frac{M}{2\pi i \Delta z} \exp[iS_{cl}], \quad (20)$$

where $\Delta z = z_2 - z_1$ and S_{cl} is the classical action for the Hamiltonian (19) given by

$$\begin{aligned}S_{cl} &= -\frac{\Delta z \epsilon^2}{2M} + \frac{M}{2\Delta z} \left[(\boldsymbol{\rho}_2 - \boldsymbol{\rho}_1)^2 + \frac{2}{M} \int_{z_1}^{z_2} dt \boldsymbol{\rho}_2 \cdot \mathbf{f}(t)(t - z_1) \right. \\ &\left. + \frac{2}{M} \int_{z_1}^{z_2} dt \boldsymbol{\rho}_1 \cdot \mathbf{f}(t)(z_2 - t) - \frac{2}{M^2} \int_{z_1}^{z_2} dt \int_{z_1}^t ds \mathbf{f}(t) \cdot \mathbf{f}(s)(z_2 - t)(s - z_1) \right].\end{aligned}\quad (21)$$

One can show that the LCPI formula (17) being rewritten in the momentum space reproduces the ω -spectrum corresponding to (16). Note that the subtraction of the \mathcal{K}_0 term in (17) corresponds to subtraction of the vacuum part from (11) for getting the synchrotron correction (16).

Note however that for RHIC and LHC conditions in our approach the energy loss spectrum can not be calculated accurately at gluon energy $\omega \lesssim 5$ GeV. Our numerical calculations show that for such soft gluons the large angle emission becomes important and the integration over the transverse momentum can not be performed accurately using the formulas based on the small angle approximation. For this reason our results on the energy loss can only be treated as qualitative estimates, rather than quantitative predictions.

We presented the formulas for the $q \rightarrow gq'$ transition. For the purely gluonic $g \rightarrow gg$ transition the calculations are similar.

3 Numerical results

For numerical calculations we should fix the z -dependence of the Lorentz force. As we have said, we assume that the external field acts a finite time/length $\sim 1/Q_s$. In our numerical calculations we take $L = 2/Q_s$. We take $Q_s = 1$ for RHIC and $Q_s = 1.4$ for LHC. This gives $L(\text{RHIC}) \approx 0.4$ fm and $L(\text{LHC}) \approx 0.28$ fm. To fix the z -dependence of the Lorentz force, which a fast parton feels at $\tau = z < L$, we use the τ -dependence

of the glasma energy density obtained in the lattice simulations by Lappi [20]. For our calculations we need only the field components transverse to the initial parton momentum. At $\tau \ll 1/Q_s$, when the electric and magnetic fields are almost parallel to the AA -collision axis [18, 19], the Lorentz force acting on a fast parton is purely transverse to the parton momentum. At such times for a unit color charge $F^2 = 2g^2\varepsilon$, where $\varepsilon = (E^2 + H^2)/2$ is the color field energy density. However, this relation is invalid at $\tau \gtrsim 1/Q_s$ when the contribution of the transverse (to the AA -collision axis) components of the color fields to the energy density becomes approximately equal to that from the components along the beam axis [20]. Since only half of these transverse fields squared contribute to the Lorentz force squared which we need (transverse to the jet direction) we can write in this regime $F^2 = g^2 3\varepsilon/2$. We will use this relation to determine the Lorentz force from the energy density obtained in [20].

The results of [20] were presented in terms of the coupling constant g and the mass parameter μ of the CGC model [13, 14] related to the saturation scale by the relation $Q_s \approx 6g^2\mu/4\pi$. Extrapolating to the continuum limit Lappi obtained $\varepsilon(\tau = 1/g^2\mu) = 0.26(g^2\mu)^4/g^2$, and at $\tau \gtrsim 1/g^2\mu$ the energy density behaves as $\sim 1/\tau$. We use the above value of $\varepsilon(\tau = 1/g^2\mu)$ to fix the normalization, and the τ -dependence of ε was obtained using the results for $g^2\varepsilon/(g^2\mu)^4$ presented in Fig. 3 of [20]. In [20] the glasma energy density has been calculated taking $g = 2$, and $g^2\mu = 2$ GeV for RHIC and $g^2\mu = 3$ GeV for LHC. Note that it gives the values of the glasma energy density at $\tau = 1/g^2\mu$ which match very well to the QGP energy density extracted within the Bjorken model with the longitudinal expansion [31] using the entropy/multiplicity ratio $dS/dy/dN_{ch}/d\eta = 7.67$ obtained in [32] and experimental multiplicities for the central $Au + Au$ collisions at $\sqrt{s} = 200$ GeV at RHIC and $Pb + Pb$ collisions at $\sqrt{s} = 2.76$ TeV at LHC. In terms of the QGP temperature it corresponds to $T_0 \approx 300$ MeV for RHIC, and $T_0 \approx 400$ MeV for LHC at $\tau_0 = 0.5$ fm. We use these parameters to fix the Lorentz force. For the coupling constant in the amplitude of the $q \rightarrow qg$ transition (10) we also take $g = 2$, i.e. $\alpha_s \approx 0.318$. Our numerical evaluations show that the results for the external fields in the A and B color states are very similar. Below we present the gluon emission spectra defined as a half-sum of the A and B contributions.

To illustrate the transverse momentum dependence of the gluon emission in Fig. 1 we plotted the distribution $dN_s/d\omega d\mathbf{q}$ scaled by its value at $\mathbf{q} = 0$ for \mathbf{q} along the x and y axes (we take the x -axis parallel to the Lorentz force, and the y -axis perpendicular to the Lorentz force) for a quark with energy $E = 50$ GeV and $\omega = 2, 5, 10$, and 25 GeV for RHIC and LHC conditions. The q_x -dependence in Fig. 1 is shown for the distribution averaged over two directions of the Lorentz force. Fig. 1 shows that the glasma correction has a complicated \mathbf{q} -dependence with a region where it is negative. The appearance of the negative $dN_s/d\omega d\mathbf{q}$ shows that a significant contribution comes from the interference of T_v and T_s amplitudes in (16). This says that the finite-size effects are very important for RHIC and LHC conditions (see below). From Fig. 1 one sees that the \mathbf{q} -distribution is rather broad, and large angle gluon emission is clearly important at $\omega \lesssim 5$ GeV. However, our approach, based on the small angle approximation, becomes inapplicable at the angles $\gtrsim 1$. For this reason for the p_T -integrated energy loss spectrum $dN_s/d\omega$ our approach can give only a rough estimate of the magnitude of the glasma contribution at $\omega \lesssim 5$

GeV. The observed significant contribution of the large angle gluon emission is somewhat unexpected. Indeed, one might naively expect that the typical transverse momenta should be $\sim Q_s$ (since the Lorentz force is $\sim Q_s^2$ and the path length is $\sim 1/Q_s$).

We evaluated the $dN_s/d\omega$ for two different prescriptions: (a) without any constraint on the transverse momentum (ignoring the fact that our formulas are inapplicable at large angles), and (b) imposing the kinematical constraint $|\mathbf{q}| < \min(\omega, E - \omega)$ (in this region the emission angles $\lesssim 1$ and our formulas are qualitatively reasonable). In Fig. 2 we plotted $\omega dN_s/d\omega$ for RHIC (left) and LHC (right) conditions for (a) (upper panels) and (b) (lower panels) prescriptions. One can see that the energy loss is concentrated at $\omega \lesssim 5$ GeV. In this region the kinematical constraint suppresses the distribution by a factor ~ 5 . It seems reasonable to assume that the results for the prescriptions (a) and (b) define an approximate uncertainty band of the energy loss due to the glasma color fields.

The results presented in Fig. 2 show that the glasma should not affect strongly the radiative energy loss for RHIC and LHC conditions. Indeed, even without the kinematical constraint the distributions shown in Fig. 2 turn out to be smaller by a factor $\sim 10 - 20$ than the contribution of the induced gluon emission in the QGP calculated in [9]. It is also seen from calculation of the total energy loss $\Delta E = \int_{\omega_{min}}^{\omega_{max}} d\omega \omega dN_s/d\omega$. Taking $\omega_{min} = m_g$ and $\omega_{max} = E_q/2$ without kinematical constraint we obtained for RHIC (LHC) $\Delta E \approx 184$ (320), 234 (414), and 276 (495) MeV for $E_q = 10, 20,$ and 50 GeV, respectively. For the same set of E_q imposing the kinematical constraint gives the values $\Delta E \approx 48$ (63), 49 (59), and 45 (39) MeV. These values were obtained for $m_g = 0.75$ GeV. To estimate the infrared sensitivity we also performed calculations for $m_g = 0.4$ GeV. In this case we obtained a rather small $\sim 10 - 20\%$ increase of ΔE . We also studied the sensitivity to the thickness L . If we choose $L = 3/Q_s$ (which is probably too large, since the glasma fields should become chaotic at such times) the energy loss increases by at most a factor $\sim 1.5 - 2$. The obtained values of ΔE are clearly small compared to that from the induced gluon emission in the QGP which gives $\Delta E \sim 5 - 15$ (10 - 30) GeV for RHIC (LHC) conditions at $E_q \sim 10 - 50$ GeV [7].

Thus our calculations demonstrate that, despite a huge Lorentz force acting on fast partons in the glasma, the effect of the glasma color tubes on parton energy loss turns out to be rather small. This smallness is due partly to strong finite-size effects. The point is that, similarly to the induced gluon emission due to multiple scattering, the synchrotron-like gluon emission is strongly suppressed when the parton path length in the field is of the order of (or smaller) the gluon formation length, L_f ¹. Physically this suppression is connected with the fact that the initial hard parton at $\tau = 0$ does not have a formed cloud of virtual gluons (with virtuality $Q \lesssim E$), and its splitting to a two parton state is simply impossible before formation of the higher Fock states in its wave function. To see more clearly how strong the finite-size effects are we calculated the finite-size suppression factor, S . We define it as a ratio $S = dN_s/d\omega / dN'_s/d\omega$, where $dN_s/d\omega$ is our ω -spectrum without kinematic constraint (17), and $dN'_s/d\omega$ is the spectrum in the approximation of zero formation length given by $dN'_s/d\omega = \int_0^L dz dN_s(z)/dz d\omega$. Here $dN_s(z)/dz d\omega$ is the probability distribution of the synchrotron-like gluon emission per unit length (also

¹The formation length of the synchrotron gluon emission for a constant \mathbf{f} can be estimated using the formula $L_f \sim \min(L_1, L_2)$, where $L_1 = 2\mu/\epsilon^2$ and $L_2 = (24\mu/\mathbf{f}^2)^{1/3}$ [27].

without kinematic constraint) for a uniform field equals to the real local field at position z . In the LCPI formulation the corresponding expression reads

$$\frac{dN_s(z)}{dzd\omega} = 2\text{Re} \int_{z_1}^{\infty} dz_2 \hat{g} [\mathcal{K}(\boldsymbol{\rho}_2, z_2 | \boldsymbol{\rho}_1, z_1) - \mathcal{K}_0(\boldsymbol{\rho}_2, z_2 | \boldsymbol{\rho}_1, z_1)] \Big|_{\boldsymbol{\rho}_1 = \boldsymbol{\rho}_2 = 0, z_1 = z}, \quad (22)$$

which should be calculated with the Hamiltonian (19) but for a constant \mathbf{f} equals to the real Lorentz force at position z . The spectrum (22) can be written in terms of the Airy function [27]. For a very large slab with a smooth z -dependence of the Lorentz force, when at each z the local gluon formation length satisfies the inequality $L_f \ll z$, the local radiation rate $dN_s(z)/dzd\omega$ becomes well defined. In this regime the factor S should become close to unity. Thus, the deviation of S from unity characterizes the strength of the finite-size effects. In Fig. 3 we plotted the suppression factor S for RHIC and LHC conditions for several quark energies. From Fig. 3 one can see that in the region $\omega \lesssim 5$ GeV dominating energy loss the finite-size effects suppress the radiation rate by a factor 3 – 5. Such strong suppression is not surprising since in this region the gluon formation length is of the order of the glasma life time.

We presented the numerical results for gluon emission from a fast quark. For a fast gluon the gluon emission spectrum $dN_s/dxd\mathbf{q}$ is symmetric in $x \leftrightarrow 1 - x$. At $x \lesssim 0.5$ it is very similar in form to that for a quark, but enhanced by a factor $\sim C_A/C_F = 9/4$.

4 Summary

In this paper we studied the synchrotron-like gluon emission induced by interaction of fast partons with the coherent color fields in the glasma phase which should exist in AA -collisions at $\tau \sim 1/Q_s$, before formation of the QGP. We modeled the glasma by a time-dependent Lorentz force acting on fast partons at $\tau \lesssim (2 - 3)/Q_s$. We evaluated the synchrotron-like gluon emission using a quasiclassical formalism based on the small angle approximation. But our numerical calculations show a significant contribution of the large angle region for gluons with $\omega \lesssim 5$ GeV which are important for the total energy loss. For this reason our study is not expected to give accurate information on the energy loss in the glasma. Nevertheless it seems relatively safe to use the results for qualitative estimate of the glasma effect on the radiative energy loss.

Our results show that for RHIC and LHC conditions despite very large values of the coherent glasma color fields the order of magnitude of the synchrotron-like energy loss turns out to be small as compared to the radiative energy loss in the QGP phase. For this reason the glasma phase should not play a significant role in the suppression of high- p_T hadrons. But due to a wide angle distribution the synchrotron-like gluon emission may potentially be important for the jet structure at large angles (such as ridge effect and conical emission). However, an accurate study of this region would require the calculations beyond the small angle approximation.

Acknowledgements

We are grateful to T. Lappi for a useful communication on his numerical simulation of the glasma. One of the authors (BGZ) would like to thank LAPTH and CERN TH

Division for hospitality and partial support during his visits there. The work of BGZ is supported in part by the Laboratoire International Associé "Physique Théorique et Matière Condensée" (ENS-Landau), the grant RFBR 12-02-00063-a and the program SS-6501.2010.2.

References

- [1] R. Baier, Y.L. Dokshitzer, A.H. Mueller, S. Peigné and D. Schiff, Nucl. Phys. B**483**, 291 (1997); *ibid.* B**484**, 265 (1997); R. Baier, Y.L. Dokshitzer, A.H. Mueller and D. Schiff, Nucl. Phys. B**531**, 403 (1998).
- [2] B.G. Zakharov, JETP Lett. **63**, 952 (1996); *ibid* **65**, 615 (1997); **70**, 176 (1999); Phys. Atom. Nucl. **61**, 838 (1998).
- [3] R. Baier, D. Schiff and B.G. Zakharov, Ann. Rev. Nucl. Part. **50**, 37 (2000) [arXiv:hep-ph/0002198].
- [4] U.A. Wiedemann, Nucl. Phys. A**690**, 731 (2001).
- [5] M. Gyulassy, P. Lévai and I. Vitev, Nucl. Phys. B**594**, 371 (2001).
- [6] P. Arnold, G.D. Moore and L.G. Yaffe, JHEP **0206**, 030 (2002).
- [7] B.G. Zakharov, JETP Lett. **86**, 444 (2007) [arXiv:hep-ph/0708.0816].
- [8] G.-Y. Qin, J. Ruppert, C. Gale, S. Jeon, G.D. Moore and M.G. Mustafa, Phys. Rev. Lett. **100**, 072301 (2008) [arXiv:0710.0605 [hep-ph]].
- [9] B.G. Zakharov, JETP Lett. **80**, 617 (2004) [arXiv:hep-ph/0410321].
- [10] B.G. Zakharov, JETP Lett. **88**, 781 (2008) [arXiv:0811.0445 [hep-ph]].
- [11] B.G. Zakharov, JETP Lett. **93**, 683 (2011) [arXiv:1105.2028 [hep-ph]].
- [12] A. Kovner, L.D. McLerran and H. Weigert, Phys. Rev. D**52**, 3809 (1995) [arXiv:hep-ph/9505320]; Phys. Rev. D**52**, 6231 (1995) [arXiv:hep-ph/9502289].
- [13] L.D. McLerran and R. Venugopalan, Phys. Rev. D**49**, 2233 (1994).
- [14] L.D. McLerran and R. Venugopalan, Phys. Rev. D**49**, 3352 (1994).
- [15] E. Iancu, A. Leonidov and L.D. McLerran, arXiv:hep-ph/0202270.
- [16] F. Gelis, E. Iancu, J. Jalilian-Marian and R. Venugopalan, Ann. Rev. Nucl. Part. Sci. **60**, 463 (2010) [arXiv:1002.0333 [hep-ph]].
- [17] T. Lappi and L.D. McLerran, Nucl. Phys. A**772**, 200 (2006) [arXiv:hep-ph/0602189].
- [18] L.D. McLerran, Acta Phys. Polon. B**41**, 2799 (2010) [arXiv:1011.3203 [hep-ph]].

- [19] T. Lappi, Int. J. Mod. Phys. E**20**, 1 (2011) [arXiv:1003.1852 [hep-ph]].
- [20] T. Lappi, Phys. Lett. B**643**, 11 (2006).
- [21] T. Lappi, Eur. Phys. J. C**71**, 1699 (2011) [arXiv:1104.3725 [hep-ph]].
- [22] H. Fujii and K. Itakura, Nucl. Phys. A**809**, 88 (2008) [arXiv:0803.0410 [hep-ph]].
- [23] P. Romatschke and R. Venugopalan, Phys. Rev. D**74**, 045011 (2006) [arXiv:hep-ph/0605045].
- [24] A. Iwazaki, Prog. Theor. Phys. **121**, 809 (2009) [arXiv:0803.0188 [hep-ph]].
- [25] C. Shen, U. Heinz, P. Huovinen and H. Song, Phys. Rev. C**82**, 054904 (2010) [arXiv:1010.1856 [nucl-th]].
- [26] H. Song, S.A. Bass, U. Heinz, T. Hirano and C. Shen, Phys. Rev. C**83**, 054910 (2011) [arXiv:1101.4638 [nucl-th]].
- [27] B.G. Zakharov, JETP Lett. **88**, 475 (2008) [arXiv:0809.0599 [hep-ph]].
- [28] N.N. Nikolaev and B.G. Zakharov, Phys. Lett. B**327**, 149 (1994).
- [29] E.V. Shuryak, Rev. Mod. Phys. **65**, 1 (1993).
- [30] R.P. Feynman and A.R. Hibbs, *Quantum Mechanics and Path Integrals*, McGRAW-HILL Book Company, New York 1965.
- [31] J.D. Bjorken, Phys. Rev. D**27**, 140 (1983).
- [32] B. Müller and K. Rajagopal, Eur. Phys. J. C**43**, 15 (2005).

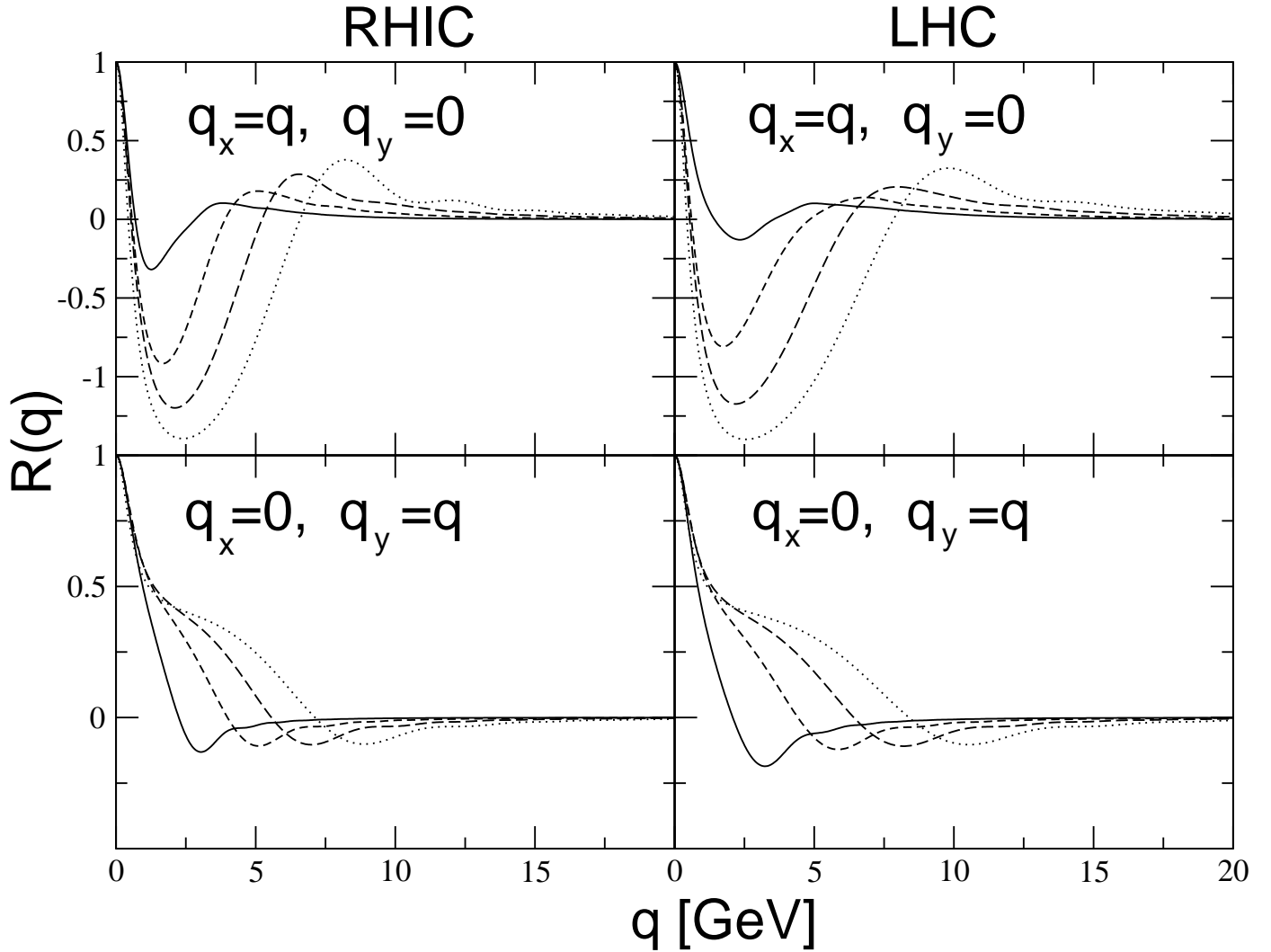


Figure 1: The ratio $R(q) = dN_s/d\omega d\mathbf{q}/dN_s/d\omega d\mathbf{q}|_{\mathbf{q}=0}$ for $q \rightarrow gq$ process at $E_q = 50$ GeV obtained using (16) for RHIC (left) and LHC (right) conditions for the gluon energies $\omega = 2$ (solid lines), 5 (short dashed lines), 10 (long dashed lines), and 25 (dotted lines) GeV. The transverse momentum vector is given by $\mathbf{q} = (q, 0)$ (upper panels), and $\mathbf{q} = (0, q)$ (lower panels), here x -axis in \mathbf{q} -plane is parallel to the Lorentz force \mathbf{f} , and y -axis is perpendicular to it.

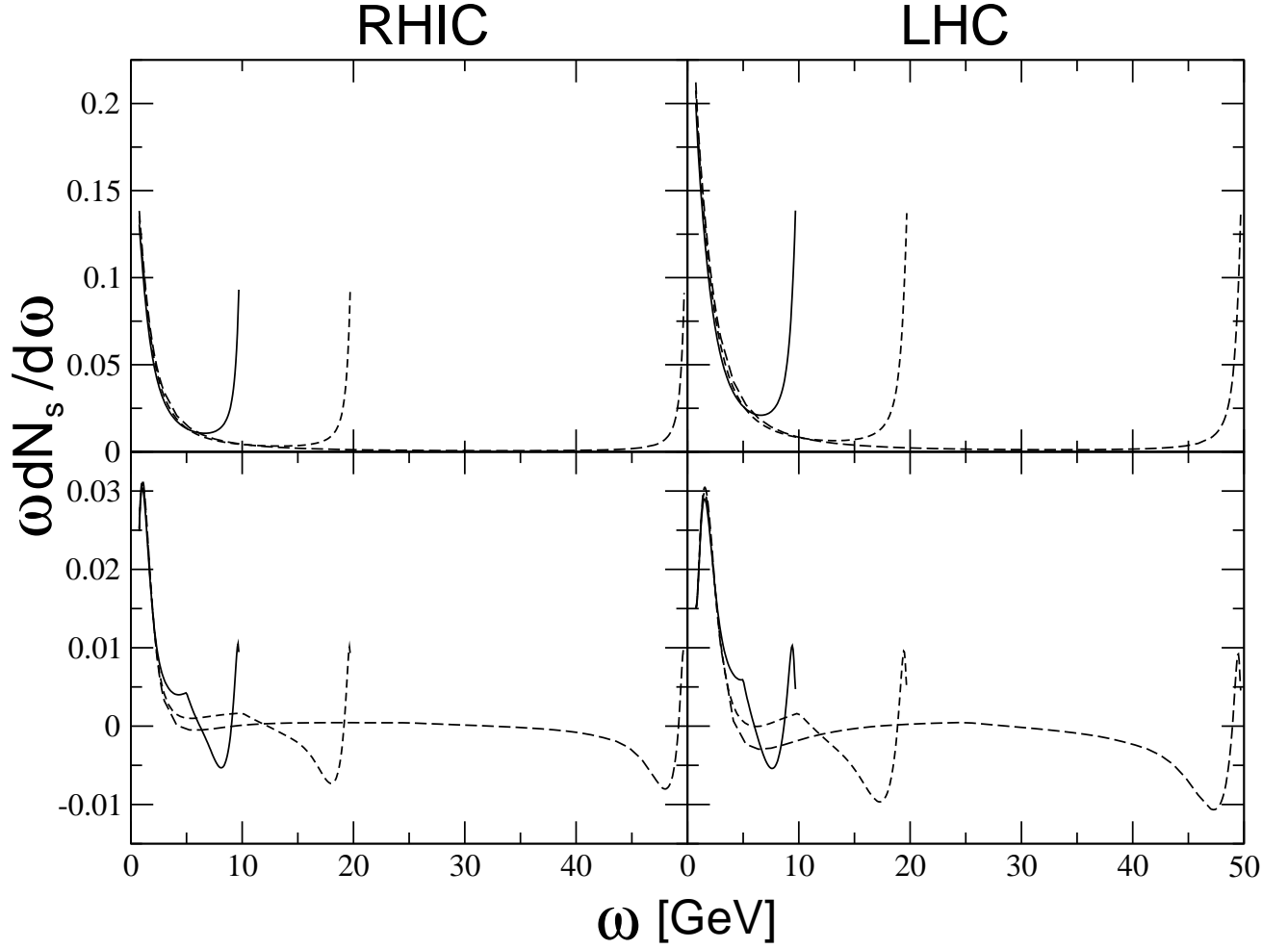


Figure 2: The energy loss spectrum $\omega dN_s/d\omega$ for $q \rightarrow gq$ process at $E_q = 10$ (solid lines), 20 (short dashed lines), and 50 (long dashed lines) GeV for RHIC (left) and LHC (right) conditions obtained from (16) without kinematical constraint on the transverse momentum (upper panels) and with the restriction $|\mathbf{q}| < \min(\omega, E - \omega)$ (lower panels).

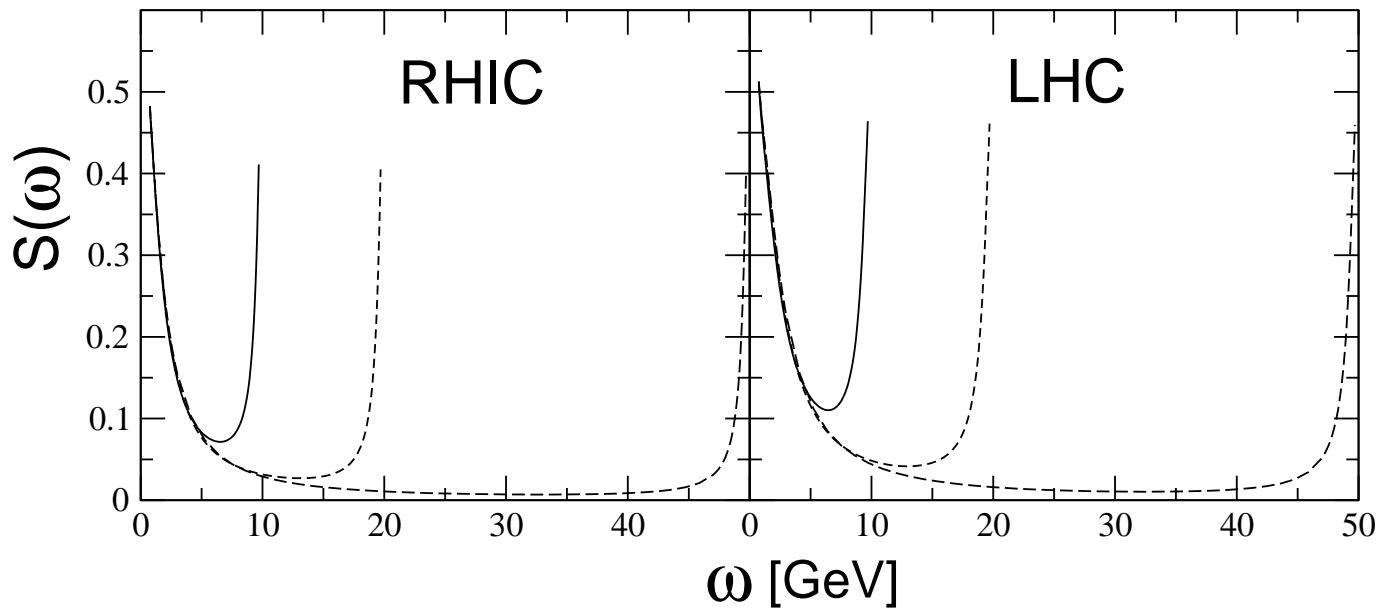


Figure 3: The finite-size suppression factor for $q \rightarrow gq$ process for RHIC (left) and LHC (right) conditions for the ω -distribution obtained without kinematical constraint on transverse momentum, see text for details. The curves are for $E_q = 10$ (solid lines), 20 (short dashed lines), and 50 (long dashed lines) GeV.